

# The $^{210}\text{Po}$ / $^{210}\text{Pb}$ disequilibrium in a spring-blooming marginal sea, the Southern Yellow Sea

Qiangqiang Zhong<sup>a</sup>, Jinlong Wang<sup>a,\*</sup>, Jinzhou Du<sup>a</sup>, Qianqian Bi<sup>a</sup>, Feng Zhao<sup>b</sup>

<sup>a</sup> State Key Laboratory of Estuarine and Coastal Research, East China Normal University, Shanghai, 200062, China

<sup>b</sup> South China Sea Environmental Monitoring Center, State Oceanic Administration, Guangzhou, 510300, China



## ARTICLE INFO

### Keywords:

$^{210}\text{Po}/^{210}\text{Pb}$

Disequilibria

Residence time

Southern Yellow sea

Particulate organic carbon

Algal blooming

## ABSTRACT

The Southern Yellow Sea (SYS) is suffering from the increasing environment problems, such as the recurrent algal bloom. The  $^{210}\text{Po}/^{210}\text{Pb}$  disequilibrium is very useful for assessing particulate organic matter dynamics during phytoplankton blooming. In this study, 23 surface samples were collected from the SYS after the 2009 spring bloom, to investigate the disequilibrium between these two radionuclides. The dissolved  $^{210}\text{Pb}$  and particulate  $^{210}\text{Pb}$  activities ( $\text{dpm } 100 \text{ L}^{-1}$ ) in the SYS surface waters varied within a wide range, with values of 2.28–17.82 (average  $7.63 \pm 4.25$ ,  $n = 23$ ) and 1.08–13.56 (average:  $4.72 \pm 2.84$ ,  $n = 23$ ). A deficiency of  $^{210}\text{Po}$  relative to  $^{210}\text{Pb}$  in the seawater was observed. The distribution coefficients ( $K_d$ ) of the two radionuclides varied considerably (from  $10^4$  to  $10^6 \text{ L kg}^{-1}$ ), and higher  $K_d$  values of  $^{210}\text{Po}$  relative to  $^{210}\text{Pb}$  generally increased with POC/TSM (when above 10%). The negative correlation ( $R = 0.97$ ,  $P = 0.012$ ) between  $^{210}\text{Po}/^{210}\text{Pb}$  activity ratios and primary productivities in all four seasons implies that marine biological processes may enhance the disequilibrium between  $^{210}\text{Po}$  and  $^{210}\text{Pb}$ . The residence times of  $^{210}\text{Po}$  and  $^{210}\text{Pb}$  were estimated to be 7–206 days and 14–105 days, respectively. The longer  $^{210}\text{Po}$  residence times might be connected with several processes, e.g.,  $^{210}\text{Po}$  uptake by marine particles or plankton, and recycling of fine-grained particles in the surface water. These short residence times of  $^{210}\text{Po}$  and  $^{210}\text{Pb}$  might indicate the existence of efficient scavenging processes, causing heavy metals and pollutants to deposit into the Yellow Sea (YS) bottom sediments.

## 1. Introduction

In marine systems,  $^{210}\text{Pb}$  (half-life: 22.3 yrs) is supplied by the in situ decay of its grandparent,  $^{226}\text{Ra}$ , in the oceanic water column, and by the atmospheric fallout  $^{210}\text{Pb}$ , produced by gaseous  $^{222}\text{Rn}$ . In shallow water columns, the contribution from the disintegration of  $^{226}\text{Ra}$  is insignificant compared to the atmospheric flux (Masqué et al., 2002). The input of dissolved  $^{210}\text{Po}$  (half-life: 138.4 d) in the upper ocean is from the decay of  $^{210}\text{Pb}$ , which is ultimately derived from atmospheric fallout, with a typical  $^{210}\text{Po}/^{210}\text{Pb}$  activity ratio in precipitation of 0.1–0.2 (Bacon et al., 1976; Masqué et al., 2002; Wang et al., 2014). Although the half-life of  $^{210}\text{Pb}$  is much longer than that of  $^{210}\text{Po}$ , disequilibrium between these two radionuclides has frequently been observed in marine environments (Bacon et al., 1976; Nozaki and Tsunogai, 1976; Masqué et al., 2002; Yang et al., 2006; Wei et al., 2015; Su et al., 2017; Ma et al., 2017). This  $^{210}\text{Po}$  deficiency is caused not only by the original  $^{210}\text{Po}/^{210}\text{Pb}$  ratio in the atmosphere, but also by the distinct difference in affinity of these radionuclides for marine particles. Due to the existence of  $^{210}\text{Po}/^{210}\text{Pb}$  disequilibria in the marine system,

the ratio has frequently been utilized to determine the export fluxes of particulate organic carbon (POC) (Murray et al., 2005; Stewart et al., 2007; Wei et al., 2011, 2012; Roca-Martí et al., 2016; Su et al., 2017; Subha Anand et al., 2018).

$^{210}\text{Po}$  is preferentially taken up by marine organisms, like phytoplankton and zooplankton and other biogenic particulate material (Shannon et al., 1970; Heyraud et al., 1976; Fisher et al., 1983; Cherry et al., 1987; Kim, 2001; Tateda et al., 2003; Stewart et al., 2005). The affinity of  $^{210}\text{Pb}$  to particles in seawater is more strongly affected by the particle size and mineral components (Wei and Murray, 1994; Hung and Chung, 1998; Tateda et al., 2003; Theng and Mohamed, 2005). Thus, due to the higher affinity of  $^{210}\text{Po}$  for biological particles, the  $^{210}\text{Po}/^{210}\text{Pb}$  activity ratio in particles in the surface waters is generally greater than unity, whereas for the dissolved fraction it is generally less (e.g., Marsan et al., 2014; Jones et al., 2015). However, after certain biological processes, such as spring blooms, the distribution and fate of  $^{210}\text{Po}$  and  $^{210}\text{Pb}$  (representatives of heavy metals and pollutants) is not clear.

Biological processes, such as spring blooms may affect the

\* Corresponding author.

E-mail address: [jlwang@sklec.ecnu.edu.cn](mailto:jlwang@sklec.ecnu.edu.cn) (J. Wang).

ecosystem's carbon fixation, and its fishery industry (Tang et al., 2013). The YS, a shallow semi-enclosed marginal sea of the northwestern Pacific Ocean, has seen considerable environmental research interest recently. During recent decades, the YS has suffered a great large pollution burden, due to the substantial developments carried out along the coast of the Chinese mainland and the Korean peninsula. This pollution has included eutrophication and harmful algal blooms (Liu et al., 2017). Green tide blooms have occurred in the SYS recurrently since 2007, and after the spring bloom, a series of sub-bloom events take place at different areas to varying degrees (Tang et al., 2013; Zhou et al., 2015). Therefore, the SYS is a typical region for studying the distribution and fate of  $^{210}\text{Po}$  and  $^{210}\text{Pb}$  in a bloom-affected marginal sea. There have been investigations into the distribution of  $^{210}\text{Po}$  and  $^{210}\text{Pb}$  in eight surface water samples in 1990 (Nozaki et al., 1991), and seven water profiles along the edge of the YS in 1998 (Hong et al., 1999). However, harmful green-blue algal blooms have occurred continually since 2007, for example, from May to August 2009 (Su et al., 2013; Liu et al., 2017). The partition of  $^{210}\text{Po}$  and  $^{210}\text{Pb}$  between particles and solution, and the fractionation of these two radionuclides in the bloom-occurring SYS, are still unclear.

To improve our knowledge of the distribution and removal of  $^{210}\text{Po}$  and  $^{210}\text{Pb}$  after the spring bloom, this study determines the dissolved and particulate  $^{210}\text{Pb}$  and  $^{210}\text{Po}$ , total suspended matters (TSM) and POC concentrations in surface waters of the SYS. The aims are to (1) establish the distribution patterns and disequilibrium scales of  $^{210}\text{Po}/^{210}\text{Pb}$ , (2) estimate the partition coefficients of  $^{210}\text{Po}$  and  $^{210}\text{Pb}$ , and (3) evaluate the removal rates (residence times) of  $^{210}\text{Pb}$  and  $^{210}\text{Po}$  after phytoplankton blooms in the SYS. Moreover, the  $^{210}\text{Po}/^{210}\text{Pb}$  disequilibrium and the partition coefficients of these two radionuclides are compared with other observations from around the world.

## 2. Materials and methods

### 2.1. Sampling and preparation

The sampling was carried out from 29 July to 6 August 2009 in the SYS (Fig. 1) from a cruise of the R.V. *Beidou*. Around 25 L of surface

seawaters were collected using 30-L Niskin bottles mounted on a CTD rosette multi-sampler. For TSM and POC measurement, 3- to 5-L seawater samples were filtered (with pre-weighted  $0.7\ \mu\text{m}$  Whatman GF/F Glass fiber filters) immediately after sampling, and the filters were then washed 3 times with Milli-Q water to remove salt before frozen storage prior to laboratory analysis. The filter system used here was pre-combusted at  $450\ ^\circ\text{C}$  for 5 h before sample filtration, to decrease the background carbon levels. Analysis of POC concentration in the dried filter has been reported elsewhere (Wu et al., 2007). Briefly, the inorganic carbon was removed from the filter by using acid vapor (concentrated HCl) in desiccators for 48 h. The POC was then determined using a Vario ELIII CHNOS Elemental Analyzer. The analytical precision of the method was estimated to be around  $\pm 4\%$ , using triple measurement of the same sample.

### 2.2. $^{210}\text{Po}$ and $^{210}\text{Pb}$ analyses

Twenty liters of seawater was passed through a Nuclepore filter ( $0.45\ \mu\text{m}$  pore size, 142 mm diameter) to separate the particulate phase and the dissolved phase. Analysis for  $^{210}\text{Pb}$  and  $^{210}\text{Po}$  was referenced to Su et al. (2017). The filtrate sample was then acidified with concentrated HCl to pH 1–2, and spiked with a known amount of  $^{209}\text{Po}$  (No. 7299, Eckert & Ziegler Isotope Products) and stable  $\text{Pb}^{2+}$  (40.0 mg) to quantify any subsequent losses of Po and Pb. 100 mg of  $\text{Fe}^{3+}$  was added to the solution, and after 6–12 h of spike equilibrium, the pH was adjusted to approximately 8–9, using concentrated  $\text{NH}_4\text{OH}$  to accumulate Po and Pb with  $\text{Fe}(\text{OH})_3$  co-precipitation. After settling for 8–12 h, the precipitate was transferred into a 1.5-L polyethylene bottle, and stored on board for processing upon arrival on land. In the laboratory, the precipitate was centrifuged and dissolved in 6 M HCl solution in a clean Teflon beaker, and the pH was neutralized to about 1. After adding 0.3 g of ascorbic acid, 1 ml of 25% sodium citrate, and 1 mL of 20% hydroxylamine hydrochloride,  $^{210}\text{Po}$  and  $^{209}\text{Po}$  were auto-deposited onto a silver disc. The particulate sample filtrated on the membrane was digested with HF,  $\text{HNO}_3$ , and  $\text{HClO}_4$ , spiked with known quantities of  $^{209}\text{Po}$  and  $\text{Pb}^{2+}$  to monitor the recovery of  $^{210}\text{Po}$  and  $^{210}\text{Pb}$ . The plating procedure was similar to that utilized for dissolved

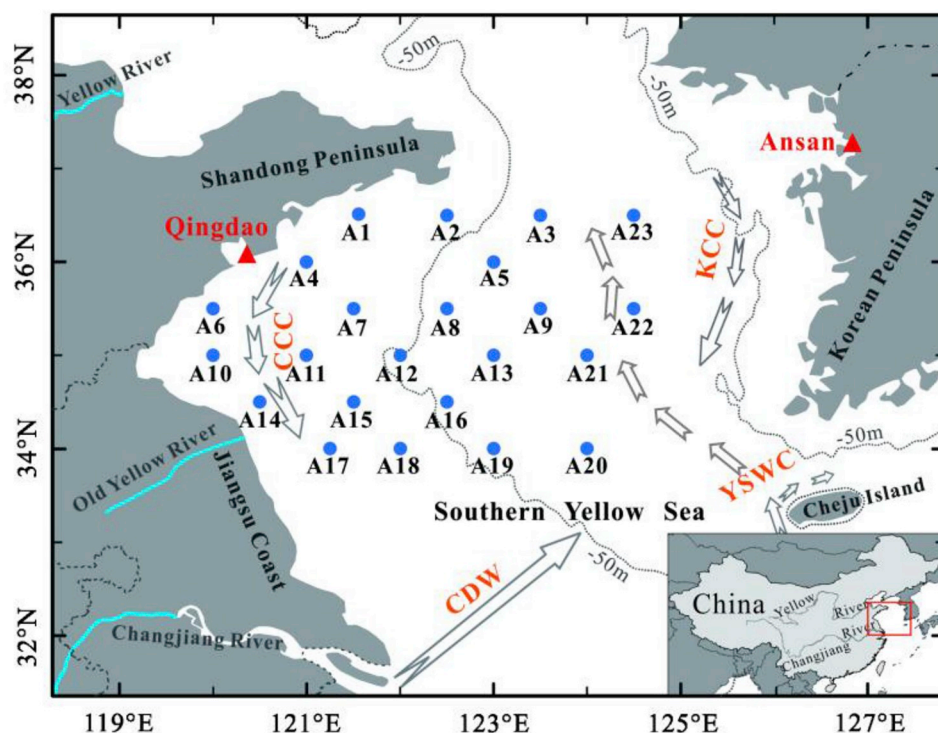


Fig. 1. Map of sampling stations in the SYS expedition during the summer of 2009. The arrows represent the general currents in the SYS in summer (Bian et al., 2013; Guo et al., 2017), these are the China Coastal Current (CCC), Korean Coastal Current (KCC), Changjiang Diluted Water (CDW), and Yellow Sea Warm Current (YSWC). The triangles are stations for measurement of the  $^{210}\text{Pb}$  atmospheric fluxes around the Yellow Sea, in Qingdao, China (Yi et al., 2005), and Ansan, Korea (Kim et al., 1998). (For interpretation of the references to colour in this figure legend, the reader is referred to the Web version of this article.)

**Table 1**  
The POC and TSM concentrations of surface waters (collected at 2 m) in the SYS.

Station code	Sampling date (mm/dd/yy)	Longitude (E°)	Latitude (N°)	Depth (m)	Temperature (°C)	Salinity	POC ( $\mu\text{M-C L}^{-1}$ )	TSM ( $\text{mg L}^{-1}$ )
A1	07/29/09	121.50	36.50	29	25.90	31.47	15.8	14.6
A2	07/29/09	122.50	36.50	20	24.48	31.12	19.5	13.4
A3	07/29/09	123.50	36.50	76	24.84	31.65	7.9	8.8
A4	07/31/09	121.00	36.00	34	25.65	31.61	13.8	14.9
A5	07/31/09	123.00	36.00	72	25.20	32.20	7.3	6.0
A6	08/01/09	120.00	35.50	27	24.12	31.51	9.5	5.3
A7	08/01/09	121.50	35.50	46	26.67	31.09	8.1	9.8
A8	08/01/09	122.50	35.50	60	25.53	31.65	7.8	8.0
A9	08/01/09	123.50	35.50	75	26.48	31.96	4.4	5.5
A10	08/02/09	120.00	35.00	23	25.88	30.78	14.2	6.4
A11	08/02/09	121.00	35.00	39	26.34	30.55	20.8	13.8
A12	08/02/09	122.00	35.00	51	26.52	31.55	9.9	9.4
A13	08/02/09	123.00	35.00	72	26.03	31.97	9.4	11.2
A14	08/03/09	120.50	34.50	16	24.74	29.96	40.5	68.1
A15	08/03/09	121.50	34.50	20	25.26	30.99	15.3	16.5
A16	08/03/09	122.50	34.50	63	25.76	31.96	7.7	8.9
A17	08/04/09	121.25	34.00	19	26.04	30.27	35.4	87.2
A18	08/04/09	122.00	34.00	27	22.40	31.60	16.2	15.1
A19	08/04/09	123.00	34.00	69	24.98	31.49	6.5	6.8
A20	08/04/09	124.00	34.00	72	24.88	30.10	8.3	NA
A21	08/05/09	124.00	35.00	76	26.48	32.17	11.4	10.3
A22	08/05/09	124.50	35.50	83	26.07	32.45	8.9	9.3
A23	08/05/09	124.50	36.50	75	24.76	30.98	8.9	8.8

NA: not available.

samples. For  $^{210}\text{Pb}$  measurement, the same sample solution was stored for  $\sim 12$  months to allow ingrowth of  $^{210}\text{Po}$  from  $^{210}\text{Pb}$ , and then polonium isotopes were auto-deposited, and counted again. The recoveries of  $^{210}\text{Pb}$  were determined through the added stable Pb and the measured Pb, using atomic absorption spectrometry (AAS). The activities of  $^{210}\text{Po}$  and  $^{210}\text{Pb}$  in the samples were decay corrected back to the time of sampling with the concerned factors (Church et al., 2012; Baskaran et al., 2013).

### 3. Results and discussion

#### 3.1. Distribution of water quality parameters in the SYS

The surface water temperature in the SYS between 29 July and 6 August 2009 ranged from 22.40 to 26.67 °C (Table 1). Salinity varied from 29.96 to 32.45, with high values in the central SYS, and low values in coastal regions, especially near the southwest coast (Fig. 2), which was presumably influenced by the Changjiang River plume (Bai et al., 2014; Kim et al., 2009). The YSWC flows northwestward from the

southwest of the Cheju Island, and it seems to share the same source as the Tsushima Warm Current that both originate from the Kuroshio Current (KC) (Quan et al., 2013). The mixing of the high temperature-salinity YSWC and the low temperature-salinity Coastal Current waters results in the distribution patterns of temperature and salinity in the SYS.

The similar distribution patterns of TSM and POC concentrations in the SYS surface waters are shown in Table 1 and Fig. 3. The concentration of TSM ranged from 5.3 to 87.2  $\text{mg L}^{-1}$ , with an average of  $16.3 \pm 20.4$  ( $n = 22$ )  $\text{mg L}^{-1}$ . The POC concentrations varied from 4.4 to 40.5  $\mu\text{M-C L}^{-1}$ , with an average value of  $13.6 \pm 8.9$  ( $n = 23$ )  $\mu\text{M-C L}^{-1}$ . The highest values of TSM and POC were both observed along the northern Jiangsu Coast (TSM > 50  $\text{mg L}^{-1}$ , POC > 15  $\mu\text{M-C L}^{-1}$ ) and decreased offshore (TSM < 10  $\text{mg L}^{-1}$ , POC < 12  $\mu\text{M-C L}^{-1}$ ).

#### 3.2. The spatial distribution of $^{210}\text{Po}$ and $^{210}\text{Pb}$ in the surface water

The activities of  $^{210}\text{Pb}$  and  $^{210}\text{Po}$  in the SYS surface seawater are shown in Appendix Table A and Fig. 4. The dissolved  $^{210}\text{Pb}$  ( $^{210}\text{Pb}_d$ )

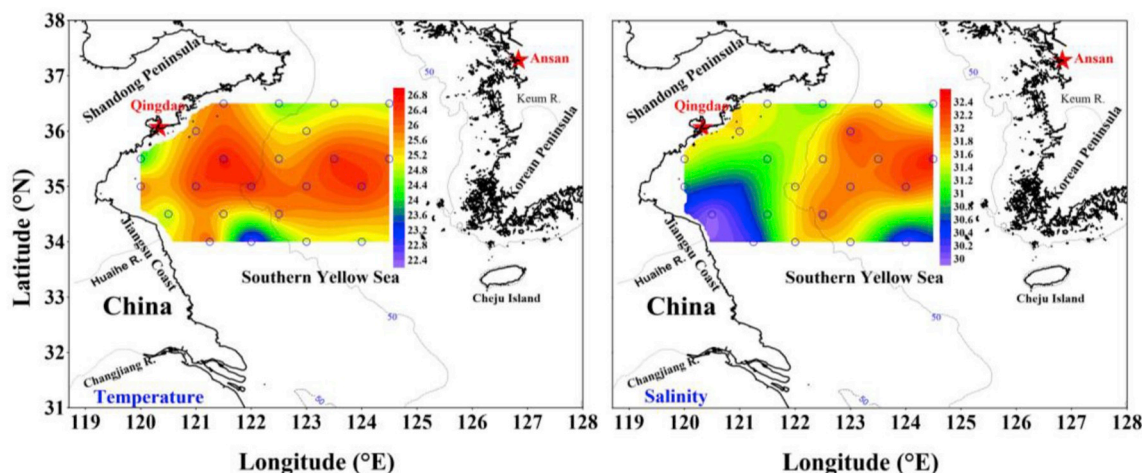


Fig. 2. Distributions of water temperature (°C) and salinity in the SYS surface waters during summer 2009 cruise.

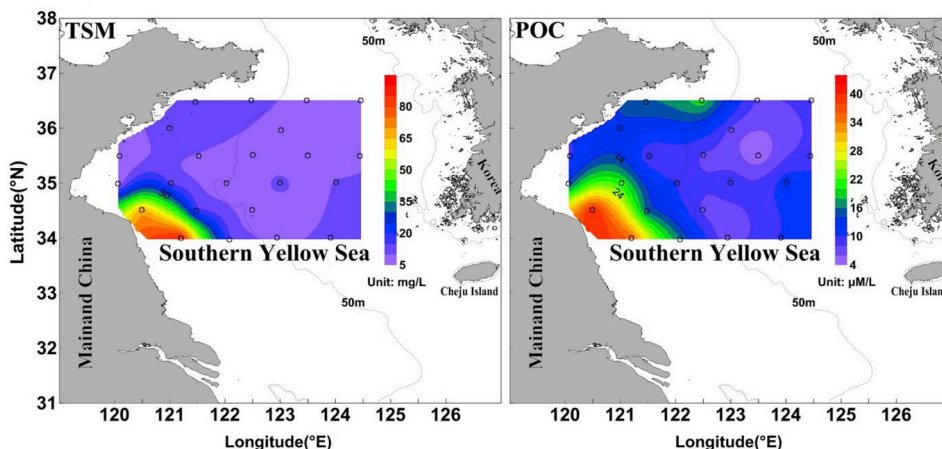


Fig. 3. Spatial distribution of TSM and POC concentrations in the SYS during summer 2009.

activities in the SYS surface water ranged from 2.28 to 17.8 dpm 100 L<sup>-1</sup>. The lower concentration of <sup>210</sup>Pb<sub>d</sub> was found in the nearshore water close to Jiangsu Coast and the Old Yellow River delta, while it increased offshore. The activities of particulate <sup>210</sup>Pb (<sup>210</sup>Pb<sub>p</sub>) were lower relative to <sup>210</sup>Pb<sub>d</sub>, and showed a variable distribution, with values of 1.08–13.6 dpm 100 L<sup>-1</sup>. The higher values of <sup>210</sup>Pb<sub>p</sub> activity were observed in the central SYS and the lower values were found at the nearshore water of Jiangsu Coast and Shandong Peninsula.

The activities of dissolved <sup>210</sup>Po (<sup>210</sup>Po<sub>d</sub>) and particulate <sup>210</sup>Po (<sup>210</sup>Po<sub>p</sub>) varied within a relatively small range, with values of 0.42–3.48 (average: 1.52 dpm 100 L<sup>-1</sup>) and 0.06–8.64 (average: 2.18 dpm 100 L<sup>-1</sup>), respectively. The activities of <sup>210</sup>Po<sub>d</sub> were generally lower than those of <sup>210</sup>Po<sub>p</sub>. The <sup>210</sup>Po<sub>d</sub> showed an irregular distribution and the <sup>210</sup>Po<sub>p</sub> was higher in the coastal areas, both off China and close to

the Korean Peninsula.

The total <sup>210</sup>Pb activities (<sup>210</sup>Pb<sub>t</sub>) varied from 5.34 to 21.66 dpm 100 L<sup>-1</sup>, with an average value of 12.35 ± 0.45 dpm 100 L<sup>-1</sup> (n = 23), which are comparable to the reported values (2.5–20.8 dpm 100 L<sup>-1</sup>) in other regions of the Chinese seas (Nozaki et al., 1991, 1998; Yang et al., 2006; Wei et al., 2015). However, the total <sup>210</sup>Po activities (<sup>210</sup>Po<sub>t</sub>) are much higher than the reported values (0.8–3.5 dpm 100 L<sup>-1</sup>) in the SYS region approximately 20 years ago (Nozaki et al., 1991). For comparison, a summary of <sup>210</sup>Pb and <sup>210</sup>Po data from shallow sea areas available from the literature is given in Table 2. Compared with other highly-turbid waters, the <sup>210</sup>Pb and <sup>210</sup>Po activities in the SYS fell within a moderate range, indicating some variability of scavenging efficiency of these radionuclides in the water.

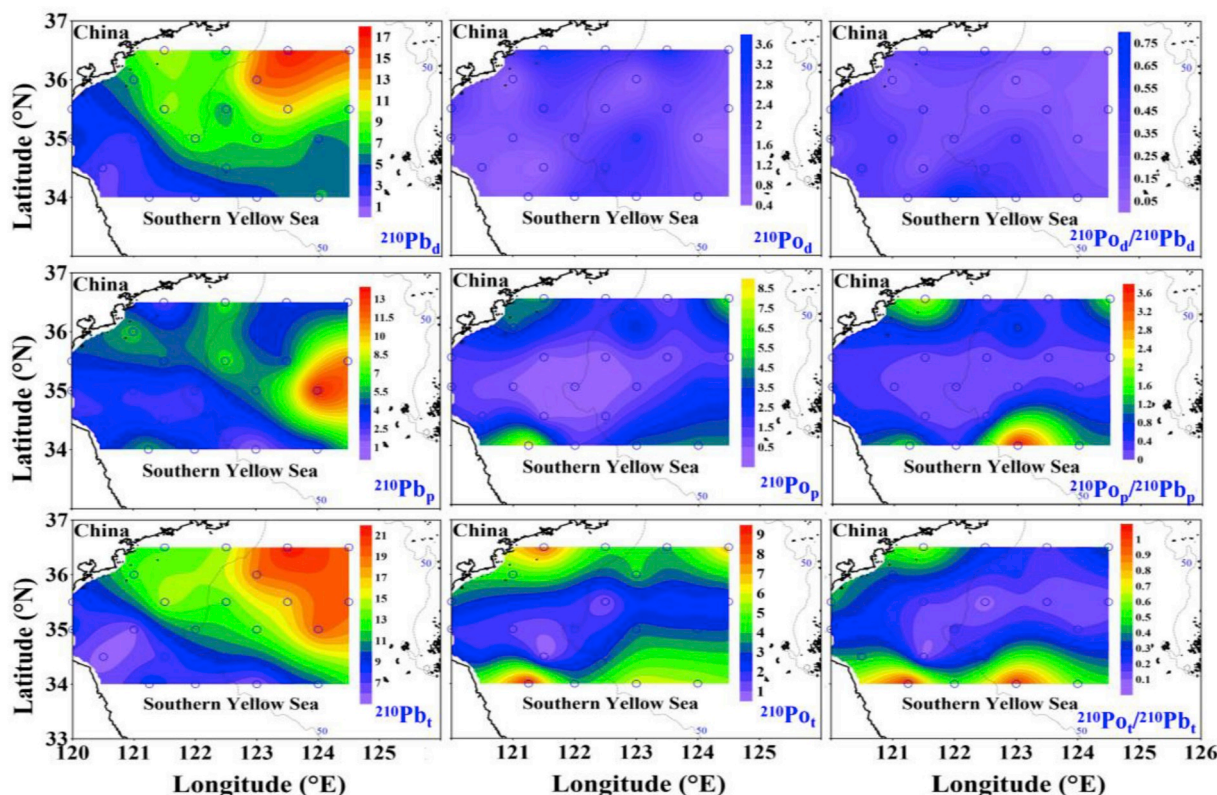


Fig. 4. Spatial distribution patterns of <sup>210</sup>Pb, <sup>210</sup>Po and the <sup>210</sup>Po/<sup>210</sup>Pb ratio in the SYS during the 2009 summer cruise (dpm 100 L<sup>-1</sup>): dissolved (d), particulate (p), and total (t).

**Table 2**  
Summary of TSM, dissolved and particulate  $^{210}\text{Po}$  and  $^{210}\text{Pb}$  activity range (average and dataset number) measured from different surface seawaters.

Location	TSM $\text{mg L}^{-1}$	$^{210}\text{Pb}_d$			$^{210}\text{Pb}_p$			$^{210}\text{Po}_d$			$^{210}\text{Po}_p$			References
		dpm $100\text{ L}^{-1}$			dpm $100\text{ L}^{-1}$			dpm $100\text{ L}^{-1}$			dpm $100\text{ L}^{-1}$			
SYS	5.3–87.2 (16.3, n = 23)	2.3–17.8 (7.6, n = 23)	1.1–13.6 (4.7, n = 23)	0.4–3.5 (1.5, n = 23)	1.1–13.6 (4.7, n = 23)	0.4–3.5 (1.5, n = 23)	0.1–8.6 (2.2, n = 23)	0.4–3.5 (1.5, n = 23)	1.1–13.6 (4.7, n = 23)	0.1–8.6 (2.2, n = 23)	0.4–3.5 (1.5, n = 23)	0.1–8.6 (2.2, n = 23)	This study	
Surrounding Taiwan	1.2–21.2 (4.1, n = 13)	1.6–7.4 (3.5, n = 13)	0.9–7.7 (3.3, n = 13)	1.2–4.8 (2.6, n = 13)	0.9–7.7 (3.3, n = 13)	1.2–4.8 (2.6, n = 13)	1.2–4.4 (2.5, n = 13)	1.2–4.8 (2.6, n = 13)	0.9–7.7 (3.3, n = 13)	1.2–4.4 (2.5, n = 13)	1.2–4.8 (2.6, n = 13)	1.2–4.4 (2.5, n = 13)	Wei et al. (2015)	
Off Taiwan coastline	1.1–7.3 (2.8, n = 15)	2.4–5.2 (3.8, n = 14)	1.0–3.2 (1.8, n = 15)	0.8–3.4 (2.1, n = 15)	1.0–3.2 (1.8, n = 15)	0.8–3.4 (2.1, n = 15)	1.1–2.9 (1.9, n = 15)	0.8–3.4 (2.1, n = 15)	1.1–2.9 (1.9, n = 15)	1.1–2.9 (1.9, n = 15)	0.8–3.4 (2.1, n = 15)	1.1–2.9 (1.9, n = 15)	Wei et al. (2012)	
Kuala Selangor Estuary, Malaysia	19.1–4005 (965.1, n = 42)	0.2–1.5 (1.1, n = 42)	0.8–1675 (394.9, n = 40)	0.1–6.7 (2.0, n = 42)	0.8–1675 (394.9, n = 40)	0.1–6.7 (2.0, n = 42)	3.0–1405 (217.3, n = 41)	0.1–6.7 (2.0, n = 42)	0.8–1675 (394.9, n = 40)	3.0–1405 (217.3, n = 41)	0.1–6.7 (2.0, n = 42)	3.0–1405 (217.3, n = 41)	Theng and Mohamed (2005)	
Jinhae Bay, Korea	2.9–37.8 (9.3, n = 7)	1.3–5.3 (2.4, n = 27)	4.6–59.1 (23.6, n = 27)	0.5–8.9 (6.6, n = 7)	4.6–59.1 (23.6, n = 27)	0.5–8.9 (6.6, n = 7)	0.5–4.5 (2.7, n = 7)	0.5–8.9 (6.6, n = 7)	4.6–59.1 (23.6, n = 27)	0.5–4.5 (2.7, n = 7)	0.5–8.9 (6.6, n = 7)	0.5–4.5 (2.7, n = 7)	Kim and Yang (2004)	
Mouth of Yellow Sea	4.4–96.3 (30.2, n = 27)	1.2–15.6 (5.3, n = 10)	0.6–24 (10.3, n = 8)	0.1–94.9 (6.8, n = 19)	0.6–24 (10.3, n = 8)	0.1–94.9 (6.8, n = 19)	1.2–64.3 (22.2, n = 27)	0.1–11.1 (3.3, n = 27)	0.6–24 (10.3, n = 8)	1.2–64.3 (22.2, n = 27)	0.1–11.1 (3.3, n = 27)	1.2–64.3 (22.2, n = 27)	Hong et al. (1999)	
Tagus estuary, Portugal	5.0–39 (20.3, n = 10)	0.1–94.9 (6.8, n = 19)	0.6–38.7 (11.4, n = 19)	0.1–94.9 (6.8, n = 19)	0.6–38.7 (11.4, n = 19)	0.1–94.9 (6.8, n = 19)	5.0–27.6 (12.1, n = 9)	0.1–8.7 (3.1, n = 11)	0.6–38.7 (11.4, n = 19)	5.0–27.6 (12.1, n = 9)	0.1–8.7 (3.1, n = 11)	5.0–27.6 (12.1, n = 9)	Carvalho (1997)	
Texas bays, USA	1.4–15.8 (7.1, n = 33)	0.2–16.8 (1.9, n = 33)	0.5–13.4 (2.8, n = 33)	0.2–16.8 (1.9, n = 33)	0.5–13.4 (2.8, n = 33)	0.2–16.8 (1.9, n = 33)	1.1–9.9 (3.2, n = 33)	0.8–21.9 (3.1, n = 33)	0.5–13.4 (2.8, n = 33)	1.1–9.9 (3.2, n = 33)	0.8–21.9 (3.1, n = 33)	1.1–9.9 (3.2, n = 33)	Baskaran and Santschi (1993)	
North Sea	3.0–10.5 (4.4, n = 16)	0.9–11.5 (5.25, n = 6)	2.7–17.6 (5.38, n = 6)	0.9–11.5 (5.25, n = 6)	2.7–17.6 (5.38, n = 6)	0.9–11.5 (5.25, n = 6)	0.7–8.6 (5.3, n = 8)	0.0–4.9 (1.5, n = 8)	0.9–11.5 (5.25, n = 6)	0.7–8.6 (5.3, n = 8)	0.0–4.9 (1.5, n = 8)	0.7–8.6 (5.3, n = 8)	Zuo and Eisma (1993)	
Narragansett Bay, USA													Santschi et al. (1979)	

### 3.3. The sources and sinks of $^{210}\text{Pb}$ and $^{210}\text{Po}$ in sea surface waters

Generally, the levels of  $^{210}\text{Pb}$  and  $^{210}\text{Po}$  in the ocean surface waters are dominated by their sources (i.e., atmospheric depositional flux, mixing) and sinks (particle scavenging and sinking, mixing and radioactive decay) (Nozaki et al., 1976). In the shallow SYS, the influence from the very thin mixed layer is expected to be small. The input of riverine  $^{210}\text{Pb}$  to the coastal and shelf waters could also be negligible because of the fast scavenging and settling of  $^{210}\text{Pb}$  by riverine suspended particles, and high-efficiency trapping of sediments in estuaries (Benninger, 1978). For example, in the Changjiang Estuary the scavenging rate constants of  $^{210}\text{Pb}$  were high ( $0.07\text{--}0.11\text{ day}^{-1}$ ) and the residence times of  $^{210}\text{Pb}$  were short (8–15 days) relative to those in coastal and shelf areas (Huang et al., 2013); and it has been estimated that almost 100% of the  $^{210}\text{Pb}$  from the Changjiang was trapped in the estuary (Wang et al., 2018). Thus, the main source of  $^{210}\text{Pb}$  in the SYS should be attributed to atmospheric deposition. The atmospheric deposition fluxes of  $^{210}\text{Pb}$  were discrepant between the China Coast and the Korean Peninsula (Fig. 1), with a low value of  $26.1\text{ dpm m}^{-2}\text{ d}^{-1}$  in Qingdao during summer (Yi et al., 2005), but a much higher value ( $237\text{ dpm m}^{-2}\text{ d}^{-1}$ ) in Ansan during summer (Kim et al., 1998).

An additional lateral supply of  $^{210}\text{Pb}$  to the higher  $^{210}\text{Pb}_t$  offshore surface waters in the SYS might be due to inputs from the intrusion of the YSWC water and KC (Nozaki et al., 1991; Hong et al., 1999; Quan et al., 2013). This lateral mixing contribution to the Yellow Sea and Bohai Sea (with a surface area of around  $4.2 \times 10^5\text{ km}^2$ , Hong et al., 1999) could be calculated from the influx of Kuroshio water ( $\sim 6 \times 10^{12}\text{ m}^3\text{ yr}^{-1}$ , Hong et al., 1999) and specific activity of  $^{210}\text{Pb}$  in the Kuroshio Water ( $26.6\text{ dpm }100\text{ L}^{-1}$ , Nozaki et al., 1991). The atmospheric flux of  $^{210}\text{Pb}$  input into the YS was calculated to be  $6.43 \times 10^{13}\text{ Bq yr}^{-1}$  (annual average depositional flux of  $^{210}\text{Pb}$ :  $153\text{ Bq m}^{-2}\text{ yr}^{-1}$ , Yi et al., 2005), or  $10.42 \times 10^{13}\text{ Bq yr}^{-1}$  (annual average depositional flux of  $^{210}\text{Pb}$ :  $248\text{ Bq m}^{-2}\text{ yr}^{-1}$ , Kim et al., 1998). Using these data, the contribution of the YSWC lateral input flux of  $^{210}\text{Pb}$  to the YS was estimated to be  $\sim 25\text{--}45\%$  of the atmospheric input flux.

Particle scavenging serves as an important sink for  $^{210}\text{Po}$  and  $^{210}\text{Pb}$ . As seen in Fig. 5A–D, both the TSM and POC concentrations systematically decreased toward the deeper region, and a  $^{210}\text{Po}$  deficiency relative to  $^{210}\text{Pb}$  was observed. In the nearshore shallow waters ( $< 50\text{ m}$ ), the variation of  $^{210}\text{Pb}_t$  was consistent with that of  $^{210}\text{Po}_t$ , but in the offshore waters of the SYS it was reversed (Fig. 5D). This significant difference in distribution between the nearshore and offshore region implies that both  $^{210}\text{Po}$  and  $^{210}\text{Pb}$  experience complex scavenging mechanisms. The relatively higher TSM and POC concentrations in the nearshore surface waters could support stronger  $^{210}\text{Pb}$  and  $^{210}\text{Po}$  removal processes, via sorption and subsequent sinking with clay particles (Wei and Murray, 1994; Hung and Chung, 1998; Tateda et al., 2003; Theng and Mohamed, 2005) and bio-debris derived from spring blooms in the SYS. In the offshore waters, the concentration of  $^{210}\text{Pb}$  in the dissolved phase was higher. The concentrations of clay particles and aeolian dust were low, leading to less  $^{210}\text{Pb}$  scavenged from the water column and consequently, the total  $^{210}\text{Pb}$  concentration in the offshore showed higher levels (see Fig. 4). To some extent, the POC/TSM (%) ratio can describe the composition of the particles. However, all stations showed very low values of POC/TSM for particles (below 3%, Fig. 5C), which indicates that the amount of particulate matter could be more important than its carbon content in scavenging these two nuclides in the SYS.

In the SYS surface water,  $^{210}\text{Po}$  is mainly derived from radioactive disintegration from the in-situ  $^{210}\text{Pb}$  in the water and atmospheric deposition (10–20% of  $^{210}\text{Pb}$  depositional fluxes, Bacon et al., 1976; Wang et al., 2014). It is removed from the water by particle scavenging and downward settling. Hence, the  $^{210}\text{Po}_d$  and  $^{210}\text{Po}_t$  concentrations were generally lower than those of  $^{210}\text{Pb}_d$  and  $^{210}\text{Pb}_t$  (see Fig. 4). However, possible preferential scavenging of  $^{210}\text{Po}$  by biological particles (i.e., marine bacteria, plankton cells or detritus) (Shannon et al., 1970;

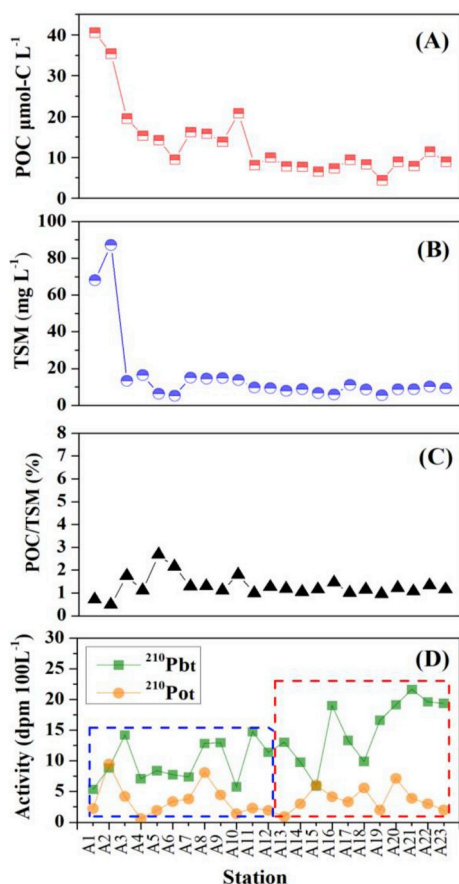


Fig. 5. Variations of TSM (A), POC (B), POC/TSM (C), and  $^{210}\text{Pb}$  and  $^{210}\text{Po}$  (D) in the surface waters of the SYS.

Heyraud et al., 1976; Fisher et al., 1983; Tateda et al., 2003; Stewart et al., 2005, 2007; Wei et al., 2015) was distinguished due to the presence of excess  $^{210}\text{Po}$  relative to  $^{210}\text{Pb}$  in the particulate phase ( $^{210}\text{Po}_p/^{210}\text{Pb}_p > 1$  at stations A1, A17, A19, A20 and A23; Appendix Table A).

### 3.4. $^{210}\text{Po}/^{210}\text{Pb}$ disequilibrium and its implications for biological processes

The degree of disequilibrium of  $^{210}\text{Po}$  relative to  $^{210}\text{Pb}$  is depicted as  $^{210}\text{Po}_v/^{210}\text{Pb}_v$  ratio. The  $^{210}\text{Po}_v/^{210}\text{Pb}_v$  ratio in surface waters of the SYS ranged from 0.07 to 1.07 (Fig. 4 and Appendix Table A), which lies within the range of  $< 0.3$  to  $\sim 1$  measured in other seas around the world (Bacon et al., 1976; Nozaki et al., 1976; Masqué et al., 2002; Murray et al., 2005; Stewart et al., 2007; Yang et al., 2006; Wei et al., 2011, 2012, 2015; Roca-Martí et al., 2016; Ma et al., 2017; Su et al., 2017; Subha Anand et al., 2018). The values of  $^{210}\text{Po}_d/^{210}\text{Pb}_d$  were less than 0.7 at all 23 stations, whereas  $^{210}\text{Po}_p/^{210}\text{Pb}_p$  ratios were greater, with the largest values of exceeding unity at 5 stations (2.17 for A1, 1.50 for A17, 3.90 for A19, 1.29 for A20, and 1.64 for A23; Fig. 4). The disequilibrium of  $^{210}\text{Po}$  relative to  $^{210}\text{Pb}$  in the dissolved phase implies a preferential scavenging of  $^{210}\text{Po}$  relative to  $^{210}\text{Pb}$ . A preferential bioaccumulation of  $^{210}\text{Po}$  rather than  $^{210}\text{Pb}$  by plankton is supported by experimental results both in the field (Shannon et al., 1970) and in the laboratory (Stewart et al., 2005).

The  $^{210}\text{Po}_v/^{210}\text{Pb}_v$  ratio ranged from low ( $< 0.25$ ) values in the central region, to slightly higher than unity ( $> 1.03$ ) in the southern part of the SYS. Combined with published data on the SYS, a significant correlation ( $R = 0.97$ ,  $P = 0.012$ ) is found between  $^{210}\text{Po}_v/^{210}\text{Pb}_v$  activity ratios and primary productivities in all four seasons (see Fig. 6), which implies that strong marine biological activities might facilitate

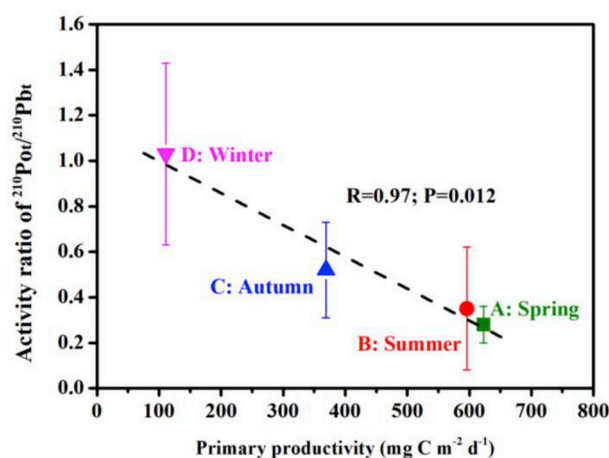


Fig. 6. Plot of the average values of the  $^{210}\text{Po}_v/^{210}\text{Pb}_v$  activity ratio versus primary productivities in the SYS: A) spring ( $n = 8$ ; Nozaki et al., 1991); B) summer ( $n = 23$ ; this study); C) autumn ( $n = 19$ ; Ma, 2013); D) winter ( $n = 26$ ; Hong et al., 1999). The primary productivity data is cited from Zhu et al. (1993) and Liu et al. (2009).

the disequilibrium of  $^{210}\text{Po}$  and  $^{210}\text{Pb}$  in the SYS. During the rapid growth seasons, i.e. spring and summer,  $^{210}\text{Po}$  is easily enriched by marine organisms; after the plankton die, the debris and fecal pellets carrying  $^{210}\text{Po}$  sink to the seafloor, which causes an intensified disequilibrium between  $^{210}\text{Po}$  and  $^{210}\text{Pb}$  in the upper water column. However, in autumn and winter, the growth level of marine biota in the SYS is low, which leads to a weakened  $^{210}\text{Po}$  scavenging process. In addition, the vertical mixing process becomes stronger in winter (Hong et al., 1999), which might return the  $^{210}\text{Po}$  and  $^{210}\text{Pb}$  from the bottom back to the sea surface, but in this scenario, these two radionuclides might be close to equilibrium state after several months of stay at the bottom of the water column.

The export efficiency of the marine biological carbon pump ( $f$  value) is defined as the ratio between export production (EP or POC flux) and primary production (PP), which represents the strength of the carbon pump. Suppose that the  $f$  value is constant for the SYS; then the export production is proportional to primary production ( $\text{EP} \propto \text{PP}$ ). As seen in Fig. 6, the activity ratios of  $^{210}\text{Po}_v/^{210}\text{Pb}_v$  were strongly associated with primary production values ( $^{210}\text{Po}_v/^{210}\text{Pb}_v \propto \text{PP}$ ). Therefore, it could be speculated that the disequilibrium of  $^{210}\text{Po}$  and  $^{210}\text{Pb}$  is associated with export production. If this is the case, our results may support the use of  $^{210}\text{Po}$  deficiency as a method for estimating the POC flux in marine environments. However, this inference here remains uncertain, and much more evidences is needed to prove this relationship.

### 3.5. Partitioning of $^{210}\text{Po}$ and $^{210}\text{Pb}$ between dissolved and particulate phases

The scavenging and removal rate of particle-reactive nuclides from the ocean is related to the partitioning of the nuclides between the dissolved and particulate phases. The empirical distribution coefficient ( $K_d$  value,  $\text{ml g}^{-1}$ ) is defined as:

$$K_d = \frac{A_p}{A_d} \times \frac{1}{TSM} \quad (1)$$

where  $A_p$  and  $A_d$  represent the nuclide activities in the particulate and dissolved phases, respectively.  $K_d$ - $^{210}\text{Po}$  and  $K_d$ - $^{210}\text{Pb}$  have been used as indicators of the affinity of these two radionuclides for marine particulate matter (Bacon et al., 1976; Baskaran and Santschi, 1993; Santschi et al., 1979; Wei and Murray, 1994; Hong et al., 1999; Wei et al., 2012, 2015).

The  $K_d$  of  $^{210}\text{Po}$  ranged between  $0.9 \times 10^4 \text{ ml g}^{-1}$  and  $1.3 \times 10^6 \text{ ml g}^{-1}$  (see Appendix Table A). The  $K_d$ - $^{210}\text{Po}$  values were

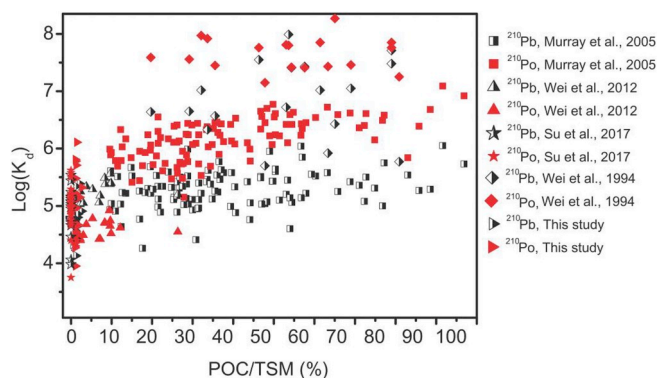


Fig. 7. Relation between  $\text{Log}(K_d)$  (for  $^{210}\text{Po}$  and  $^{210}\text{Pb}$ ) and organic carbon content (POC/TSM).

higher in the central part, and lower in the shallow domain, due to disparities in the concentration of TSM. The  $K_d$  values of  $^{210}\text{Pb}$  varied from  $1.3 \times 10^4 \text{ ml g}^{-1}$  to  $2.5 \times 10^5 \text{ ml g}^{-1}$  (Table A). These fair uniform values of  $^{210}\text{Pb}$  indicate that its distribution is less dependent on the concentration of TSM than that of  $^{210}\text{Po}$ . Both  $^{210}\text{Pb}$  and  $^{210}\text{Po}$  showed a high affinity for particulate material, as their  $\text{Log}(K_d)$  values lay mostly between 4 and 6.

The relational dataset of  $\text{Log}(K_d)$  for  $^{210}\text{Po}$  and  $^{210}\text{Pb}$  versus POC/TSM, based on our study and related literature, was collected and is summarized in Fig. 7. A clear discrepancy between distribution coefficients of  $^{210}\text{Po}$  and  $^{210}\text{Pb}$  can be discerned.  $K_d$  values for  $^{210}\text{Po}$  increased to a much higher level than those of  $^{210}\text{Pb}$  with the increase of organic carbon content. These results support the notion that  $^{210}\text{Po}$  has a greater affinity for biogenic marine particles than  $^{210}\text{Pb}$ , and can be preferentially scavenged and removed by organic particles.

Combining our data with that from the literature, we found that the  $\text{Log}(K_d-^{210}\text{Po})$  showed a negative correlation with  $\text{Log}(\text{TSM})$  in the open oceans and marginal seas ( $R = 0.64$ ,  $P < 0.00001$ ) but the relationship was much less clear in highly-turbid waters ( $R = 0.14$ ,  $P < 0.00001$ ) (Fig. 8B). By contrast, the relationship of  $\text{Log}(K_d-^{210}\text{Pb})$ - $\text{Log}(\text{TSM})$  was weak in the open oceans and marginal seas ( $R = 0.44$ ,  $P < 0.00001$ ) as well as in turbid waters ( $R = 0.32$ ,  $P < 0.00001$ ) (Fig. 8A). It is also

worth noting that the slope of  $^{210}\text{Po}$  in marginal seas and the open ocean (slope =  $-0.98$ ) tended to be lower than in turbid waters (TSM:  $> 1 \text{ mg L}^{-1}$ , slope =  $-0.21$ ). However, the slope of  $^{210}\text{Pb}$  in the marginal sea and the open ocean ( $-0.76$ ) was higher than that observed for  $^{210}\text{Po}$  at the same range of particle concentration. However, for  $^{210}\text{Pb}$  from turbid waters, the slope ( $-0.41$ ) was lower than that of  $^{210}\text{Po}$ . These results suggest that the sorption sites for  $^{210}\text{Po}$  and  $^{210}\text{Pb}$  (for a given particle concentration) may be different whether in the marginal sea, the open ocean, or turbid waters. This is probably related to particle size, particle composition, and origin of the particle (Honeyman et al., 1988).

The slope of the  $\text{Log}(K_d)$  vs.  $\text{Log}(\text{TSM})$  plot for the entire dataset was  $-0.50$  ( $R = 0.53$ ,  $P < 0.00001$ ,  $n = 986$ , Fig. 8A) for  $^{210}\text{Pb}$  and  $-0.67$  ( $R = 0.70$ ,  $P < 0.00001$ ,  $n = 890$ , Fig. 8B) for  $^{210}\text{Po}$ . Such a negative correlation between  $K_d$  and TSM can be called the “particle concentration effect” and is attributed to the presence of colloidal ligand phases in the filter-passing fraction, and particle-particle interplay (Honeyman and Santschi, 1989). Honeyman proposed that surface coordination reactions with colloids, and then colloid aggregation reactions, may play a vital role in controlling the partitioning of an element between the dissolved and particulate fractions (Honeyman et al., 1988; Honeyman and Santschi, 1989). Following Honeyman and Santschi (1989) and Wei and Murray (1994), we compiled the relationship between the mass concentration of colloids ( $C_p^*$ ) and the mass concentration of bigger, filterable particles ( $C_p$ ) for  $^{210}\text{Pb}$  ( $C_p^* = 0.50C_p - 5.53$  or  $C_p^* = f(C_p^{0.50})$ ) and  $^{210}\text{Po}$  ( $C_p^* = 0.67C_p - 5.75$  or  $C_p^* = f(C_p^{0.67})$ ) from many studies worldwide. The relationships suggest that the concentrations of filterable particles increase faster than the concentration of colloids. These results agree well with the Brownian pumping model mentioned by Honeyman and Santschi (1992), who assumed that the particle coagulation rate and the concentration of colloids ( $C_p^*$ ) should be constant for all metals in a given system. In fact, the  $C_p^*/C_p$  ratios differed for  $^{234}\text{Th}$ ,  $^{210}\text{Pb}$ , and  $^{210}\text{Po}$  in certain situations. However, the quantitative interpretation of these results is still incomplete, and it will be worthwhile to further investigate the colloidal interactions with metals of different chemical properties, and metal interactions with colloids of different compositions.

On the basis of the above discussion, the distribution behavior of  $^{210}\text{Po}$  and  $^{210}\text{Pb}$  could therefore be influenced by particle or colloid

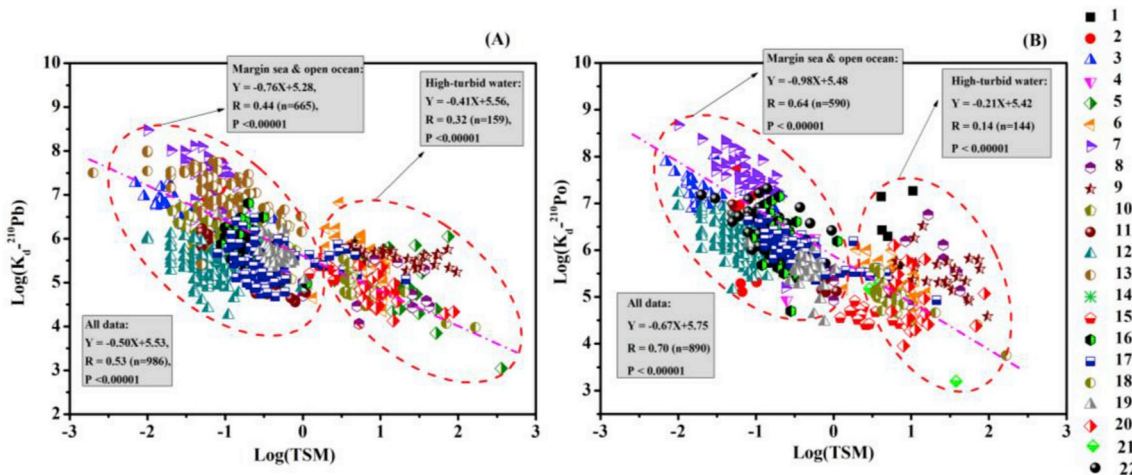


Fig. 8. Correlations of  $\text{Log}(K_d-^{210}\text{Pb})$  (A) and  $\text{Log}(K_d-^{210}\text{Po})$  (B) with  $\text{Log}(\text{TSM})$ . The  $K_d$  values were calculated from 1) Narragansett Bay, USA (Santschi et al., 1979); 2) Cariaco Trench (Bacon et al., 1980); 3) the shelf and slope south of New England (Bacon et al., 1988); 4) northeast of Taiwan, China (Yang and Lin, 1992); 5) Texas bays and Galveston's coastal waters, USA (Baskaran and Santschi, 1993); 6) southern North Sea (Zuo and Eisma, 1993); 7) Black Sea (Wei and Murray, 1994); 8) Tagus estuary, Portugal (Carvalho, 1997); 9) the mouth of the YS (Hong et al., 1999); 10) Gulf of Mexico, USA (Baskaran and Santschi, 2002); 11) northwestern Mediterranean Sea (Masqué et al., 2002); 12) the Pacific (Murray et al., 2005); 13) Chukchi Sea (Lepore et al., 2009); 14) South China Sea (Wei et al., 2011); 15) nearshore waters off Taiwan (Wei et al., 2012); 16) northern South China Sea (Wei et al., 2014); 17) surface water surrounding Taiwan (Wei et al., 2015); 18) ECS (Su et al., 2017); 19) western South China Sea (Ma et al., 2017); 20) this study; 21) Jinhae Bay, Korea (Kim and Yang, 2004); 22) Sea of Japan (Hong et al., 2008).

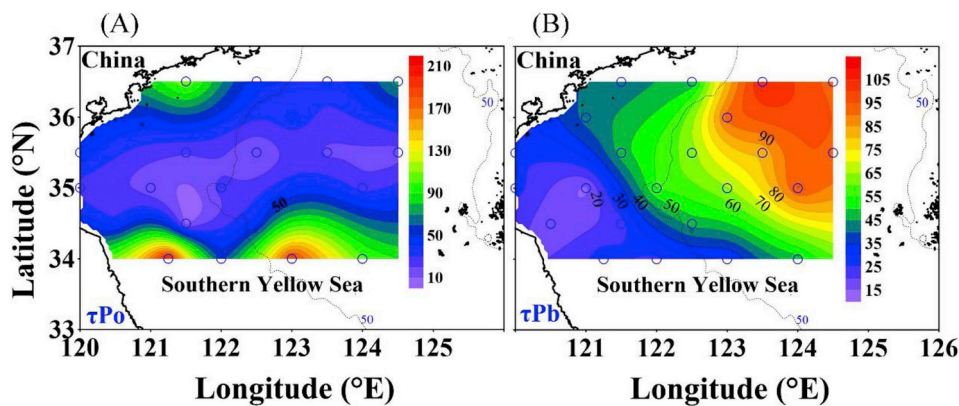


Fig. 9.  $\tau_{Po}^t$  (A) and  $\tau_{Pb}^t$  (B) in the SYS surface waters during summer 2009 (unit: days).

concentrations, particle composition, POC content, and other factors.

### 3.6. Residence times of $^{210}Pb$ and $^{210}Po$ in the surface waters of the SYS

Residence time is an important index for investigating the geochemical behaviors of  $^{210}Pb$  and  $^{210}Po$  in diverse aquatic environments. Due to the semi-enclosed nature of the SYS, physical processes such as advection and diffusion are rather weak (Naimie et al., 2001; Chang and Isoke, 2003). The residence times of the YS waters have been reported to be several years ( $\sim 5$ –6 years, Nozaki et al., 1991; Kim et al., 2005; Men and Liu, 2015). Therefore, a simple steady-state model is used to estimate the residence time for  $^{210}Po$  and  $^{210}Pb$  (Bacon et al., 1976; Masque et al., 2002; Yang et al., 2006). The equations can be designed as follows:

$$\frac{\partial Pb}{\partial t} = 0 = F_{Pb} + \lambda_{Pb} I_{Ra} - \lambda_{Pb} I_{Pb} - k_{Pb} I_{Pb} \quad (2)$$

$$\frac{\partial Po}{\partial t} = 0 = F_{Po} + \lambda_{Po} I_{Pb} - \lambda_{Po} I_{Po} - k_{Po} I_{Po} \quad (3)$$

After rearranging Eqs. (2) and (3), we obtain:

$$\lambda_{Pb} I_{Ra} + F_{Pb} = \lambda_{Pb} I_{Pb}^d + k_{Pb} I_{Pb} (J_{Pb}) \quad (4)$$

$$J_{Pb} = \lambda_{Pb} I_{Pb}^p + P_{Pb} \quad (5)$$

$$\lambda_{Po} I_{Pb}^d + F_{Po} = \lambda_{Po} I_{Po}^d + k_{Po} I_{Po} (J_{Po}) \quad (6)$$

$$\lambda_{Po} I_{Pb}^p + J_{Po} = \lambda_{Po} I_{Po}^p + P_{Po} \quad (7)$$

where Eqs. (4) and (5) are mass-balance equations for dissolved and particulate  $^{210}Pb$ , and equations (6) and (7) are mass-balance equations for dissolved and particulate  $^{210}Po$ . The residence times of  $^{210}Po$  and  $^{210}Pb$  can therefore be written as:

$$\tau_{Po}^d = I_{Po}^d / J_{Po} \quad (8)$$

$$\tau_{Po}^p = I_{Po}^p / P_{Po} \quad (9)$$

$$\tau_{Pb}^d = I_{Pb}^d / J_{Pb} \quad (10)$$

$$\tau_{Pb}^p = I_{Pb}^p / P_{Pb} \quad (11)$$

$$\tau_{Po}^t = I_{Po}^t / P_{Po} \quad (12)$$

$$\tau_{Pb}^t = I_{Pb}^t / P_{Pb} \quad (13)$$

The parameters that appear in these ten expressions are:

- (1)  $F_{Pb}$ ,  $F_{Po}$ : atmospheric fluxes of  $^{210}Pb$  and  $^{210}Po$  to the sea surface water of the SYS. The average annual atmospheric  $^{210}Pb$  flux was measured by Yi et al. (2005) in Qiangdao, China, and Kim et al.

(1998) in Ansan, Korea, at  $1.12 \text{ dpm cm}^{-2} \text{ yr}^{-1}$  and  $1.5 \text{ dpm cm}^{-2} \text{ yr}^{-1}$ , respectively. Hence, an arithmetic average of  $^{210}Pb$  atmospheric flux from these two regions was used. The annual atmospheric flux of  $^{210}Po$  is considered to be about 16.3% of that of  $^{210}Pb$  (Yi et al., 2005), due to the low residence times of  $^{210}Pb$  and  $^{210}Po$  in the lower atmosphere (Bacon et al., 1976; Masqué et al., 2002).

- (2)  $\lambda$  is the decay constant of the radionuclides  $^{210}Pb$  and  $^{210}Po$  ( $\lambda_{Pb} = 0.03108 \text{ yr}^{-1}$  and  $\lambda_{Po} = 1.833 \text{ yr}^{-1}$ ).
- (3)  $I_{Ra}$ ,  $I_{Pb}$ , and  $I_{Po}$  are the inventories of the radionuclide in the surface layer, calculated by multiplying their activities by the thickness of the surface layer. As mentioned above, the surface layer thickness was ca. 10 m at the nearshore stations and ca. 20 m at the offshore stations.
- (4)  $P_{Pb}$  and  $P_{Po}$  are the rates of particulate  $^{210}Pb$  and  $^{210}Po$  by particles sinking out of the surface layer.
- (5)  $J_{Pb}$  and  $J_{Po}$  are the rates of scavenging of  $^{210}Pb$  and  $^{210}Po$ . If a radionuclide is transferred from solution to the particulate phase by particle scavenging, then  $J$  is positive, and for the reverse process it is negative.
- (6)  $\tau^p$ ,  $\tau^d$ , and  $\tau^t$  are the residence times of the radionuclide in the particulate, dissolved and total phases.

The estimated  $\tau^p$ ,  $\tau^d$  and  $\tau^t$  for  $^{210}Po$  and  $^{210}Pb$  in the SYS are shown in Fig. 9 and Appendix Table A, which also shows uncertainties estimated by error propagation. From Fig. 9, it can clearly be observed that the  $\tau^t$  of  $^{210}Pb$  increases from nearshore ( $\sim 20$  days) to offshore waters ( $\sim 100$  days). The  $\tau^t$  of  $^{210}Po$  ranged from 7 days to 206 days, and was shorter in the central region, and longer at several other stations in the study area. The longer  $\tau^t$  of  $^{210}Po$  than that of  $^{210}Pb$  has also been observed by other studies (0.8 years for  $^{210}Pb$ , 3.0 years for  $^{210}Po$ , Masqué et al., 2002; 3–15 days for  $^{210}Pb$ , 14–125 days for  $^{210}Po$ , Wei et al., 2012). The  $\tau_{Po}^d$  and  $\tau_{Pb}^d$  were in the range of 5–46 days and 7–86 days, respectively. The lower  $\tau_{Po}^d$  relative to  $\tau_{Pb}^d$  further confirms that  $^{210}Pb$  was more slowly scavenged by particles than  $^{210}Po$ . The  $\tau_{Pb}^p$  varied from 5 days to 66 days, with an average of 20 days, which was much lower than that in the southern South China Sea ( $\sim 50$  days, Yang et al., 2006) and the North Pacific Subtropical Gyre ( $\sim 55$  days, Ma et al., 2013). These results once again prove that  $^{210}Pb$  removal in turbid waters is faster than in clean ocean waters, which is consistent with higher TSM concentrations in coastal waters. The shorter residence times of Po and Pb ( $< 0.5$  year, this study), compared with the residence time of SYS waters ( $\sim 5$ –6 years), indicate that particle-reactive matter (like Po, Pb and other particle-reactive heavy metals) is more rapidly scavenged and removed by particles in turbid coastal waters, and is largely deposited on the bottom sediments of the YS rather than transported to the pelagic sea.

Fig. 10 shows the scavenging pathways of  $^{210}Po$  and  $^{210}Pb$  in the

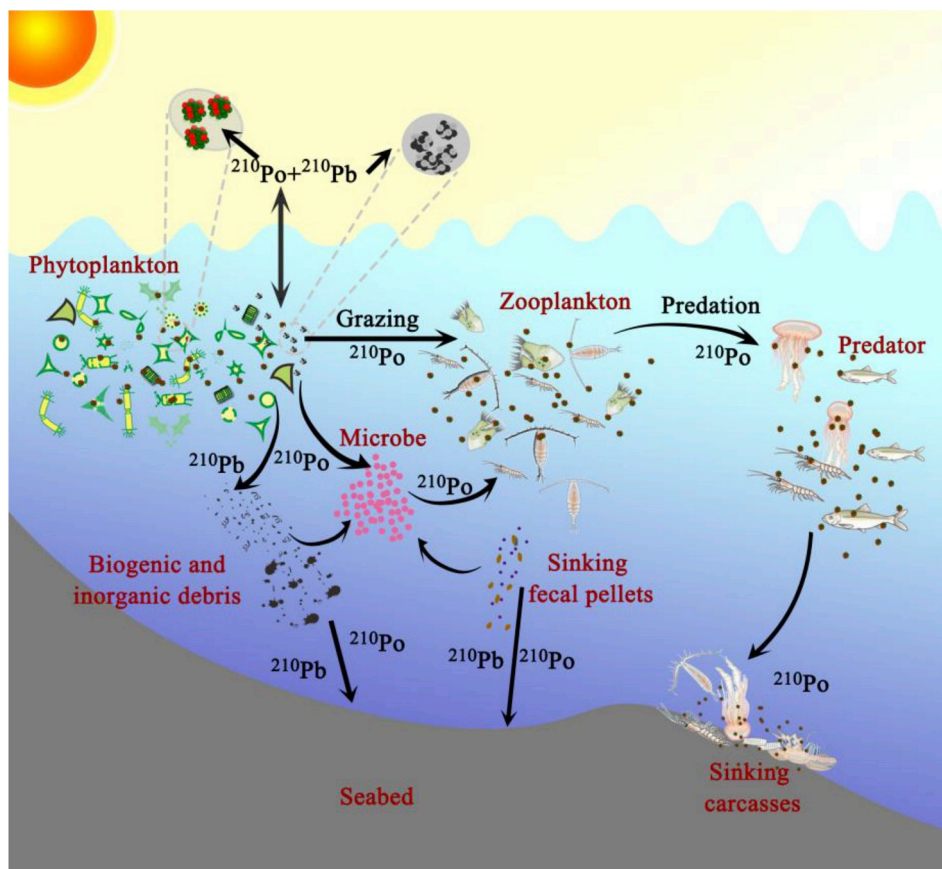


Fig. 10. Schematic diagram of  $^{210}\text{Po}$  and  $^{210}\text{Pb}$  scavenging mechanisms after phytoplankton blooms in the SY.

SYS. Both  $^{210}\text{Pb}$  and  $^{210}\text{Po}$  are efficiently enriched by phytoplankton, and fast eliminated from the surface layer due to this particle-reactive behavior. However,  $^{210}\text{Pb}$  and  $^{210}\text{Po}$  are accumulated by phytoplankton in different ways.  $^{210}\text{Pb}$  seems to adhere to the surface of cells and would not be assimilated by the marine organisms. Hence,  $^{210}\text{Pb}$  may only be removed from upper layer when associated with fecal pellets, debris, and other particles, without being effectively recycled (Masqué et al., 2002). And the dissolution of  $^{210}\text{Pb}$  from fecal pellets would be difficult (Fisher et al., 1983), even though it occurred, it would be slow. Nozaki et al. (1998) found that  $^{210}\text{Pb}$  is exported out of surface waters, usually associated with inorganic detritus. In contrast,  $^{210}\text{Po}$  can be accumulated by cell cytoplasm (Fisher et al., 1983), enters the metabolism and later can be enriched by zooplankton (Cherry et al., 1987) and recycled by microbes (Kim, 2001). It is therefore considered that  $^{210}\text{Po}$  could be scavenged and removed through fecal pellets and sink to the deep layers of the water column. Higgo et al. (1980) estimated that more than 80% of  $^{210}\text{Po}$  removal was due to the sinking of fecal pellets. Masqué et al. (2002) observed that  $^{210}\text{Po}$  would tend to be accumulated in less dense suspended matter, such as the cells of microbes, and be less liable to sink, which means that  $^{210}\text{Po}$  tends to be more efficiently adsorbed by biogenic particles due to its lower density than mineral particles. Particles with higher densities sink, but suspended matter with lower density and higher  $^{210}\text{Po}$  remains at the surface for a much longer time, leading to the longer residence times of  $^{210}\text{Po}$  in the surface water (Masqué et al., 2002).

#### 4. Conclusions

According to the spatial patterns of dissolved and particulate activities of  $^{210}\text{Pb}$ ,  $^{210}\text{Po}$ , POC and TSM concentrations in the surface waters of the southern Yellow Sea in the summer of 2009, the following conclusions can be drawn:

- 1) The activities of  $^{210}\text{Pb}_t$  and  $^{210}\text{Po}_t$  had a range of 5.3–21.7 dpm  $100\text{ L}^{-1}$  and 0.6–9.5 dpm  $100\text{ L}^{-1}$ , respectively. The activities of  $^{210}\text{Pb}_d$  (2.28–17.8 dpm  $100\text{ L}^{-1}$ ) were comparable with those of  $^{210}\text{Pb}_p$  (1.08 and 13.6 dpm  $100\text{ L}^{-1}$ ), but the  $^{210}\text{Po}_d$  (0.42–3.48 dpm  $100\text{ L}^{-1}$ ) were obviously lower than those of  $^{210}\text{Po}_p$  (0.06 and 8.64 dpm  $100\text{ L}^{-1}$ ). The  $^{210}\text{Pb}$  and  $^{210}\text{Po}$  activities in the SY were comparable with other coastal and marginal seas.
- 2) The low values of the  $^{210}\text{Po}_t/^{210}\text{Pb}_t$  ratio (from  $\sim 0.1$  to 1.07) may be due to a strong  $^{210}\text{Po}$  removal process by suspended particles. A good negative relationship between  $^{210}\text{Po}/^{210}\text{Pb}$  activity ratios and primary productivities suggests that marine biological growth processes may enhance the disequilibrium between  $^{210}\text{Po}$  and  $^{210}\text{Pb}$ .
- 3) The high  $\text{Log}(K_d)$  values of  $^{210}\text{Pb}$  and  $^{210}\text{Po}$  indicate their high affinities for particles. The  $K_d$  values of  $^{210}\text{Po}$  and  $^{210}\text{Pb}$  were influenced by particle or colloid concentrations and organic carbon contents (POC/TSM) of particles.  $K_d$  values for  $^{210}\text{Po}$  increased to a much higher level than those of  $^{210}\text{Pb}$  with the increase of organic carbon content.
- 4) The  $\tau^1$  of  $^{210}\text{Po}$  and  $^{210}\text{Pb}$  were in the range of 7–206 days and 14–105 days, respectively. The  $\tau_{pb}$  was less than 1 month in the turbid nearshore water, and about 3 months in the clear offshore surface water, which is much lower than that in the open sea or ocean.

#### Acknowledgements

This study was supported by the China Postdoctoral Science Foundation (2018T110373) and the Ministry of Science and Technology of P.R. China (2006CB400601). We would like to thank the crew of the R/V *Beidou* for their kind assistance during the sample collection.

## Appendix A. Supplementary data

Supplementary data to this article can be found online at <https://doi.org/10.1016/j.jenvrad.2019.05.017>.

## Appendix

Activities of  $^{210}\text{Pb}$  and  $^{210}\text{Po}$  in the total ( $^{210}\text{X}_t$ ), dissolved ( $^{210}\text{X}_d$ ), and particulate ( $^{210}\text{X}_p$ ) phases. X represents both Pb and Po, and A.R. indicates activity ratios. Uncertainties represent counting errors ( $\pm \sigma$ ). See Table A.

Table A

Station	$^{210}\text{Pb}$ (dpm 100 L $^{-1}$ )			$^{210}\text{Po}$ (dpm 100 L $^{-1}$ )			A.R.
	Total	Dissolved	Particulate	Total	Dissolved	Particulate	$^{210}\text{Po}_d/^{210}\text{Pb}_t$
A1	12.84 ± 0.48	10.74 ± 0.42	2.10 ± 0.12	8.10 ± 0.24	3.48 ± 0.12	2.10 ± 0.12	0.63
A2	14.22 ± 0.48	7.68 ± 0.36	6.54 ± 0.30	4.20 ± 0.06	2.58 ± 0.06	6.54 ± 0.30	0.30
A3	21.66 ± 0.84	17.82 ± 0.78	3.90 ± 0.18	3.90 ± 0.12	3.24 ± 0.12	3.90 ± 0.18	0.18
A4	12.96 ± 0.42	6.96 ± 0.30	6.00 ± 0.24	4.44 ± 0.18	0.42 ± 0.00	6.00 ± 0.24	0.34
A5	19.02 ± 0.90	15.12 ± 0.84	3.96 ± 0.18	4.14 ± 0.18	0.48 ± 0.00	3.96 ± 0.18	0.22
A6	7.74 ± 0.24	3.36 ± 0.18	4.38 ± 0.18	3.36 ± 0.12	1.92 ± 0.06	4.38 ± 0.18	0.43
A7	14.76 ± 0.48	9.78 ± 0.42	4.98 ± 0.24	2.28 ± 0.00	1.98 ± 0.00	4.98 ± 0.24	0.15
A8	13.02 ± 0.42	6.54 ± 0.30	6.48 ± 0.30	0.90 ± 0.06	0.84 ± 0.06	6.48 ± 0.30	0.07
A9	16.62 ± 0.60	12.00 ± 0.60	4.62 ± 0.18	1.98 ± 0.06	1.56 ± 0.06	4.62 ± 0.18	0.12
A10	8.40 ± 0.30	5.52 ± 0.30	2.82 ± 0.12	1.92 ± 0.06	0.9 ± 0.06	2.82 ± 0.12	0.23
A11	5.76 ± 0.18	2.88 ± 0.12	2.88 ± 0.12	1.38 ± 0.06	0.96 ± 0.06	2.88 ± 0.12	0.24
A12	11.40 ± 0.42	8.88 ± 0.42	2.52 ± 0.12	1.92 ± 0.06	1.44 ± 0.06	2.52 ± 0.12	0.17
A13	13.32 ± 0.42	7.92 ± 0.36	5.40 ± 0.24	3.30 ± 0.12	2.70 ± 0.12	5.40 ± 0.24	0.25
A14	5.34 ± 0.18	2.28 ± 0.12	3.06 ± 0.12	2.22 ± 0.06	0.84 ± 0.06	3.06 ± 0.12	0.42
A15	7.08 ± 0.24	4.38 ± 0.18	2.70 ± 0.12	0.60 ± 0.00	0.42 ± 0.00	2.70 ± 0.12	0.08
A16	9.78 ± 0.42	6.54 ± 0.36	3.24 ± 0.18	3.00 ± 0.12	2.34 ± 0.12	3.24 ± 0.18	0.31
A17	8.82 ± 0.30	3.06 ± 0.12	5.76 ± 0.24	9.48 ± 0.42	0.84 ± 0.06	5.76 ± 0.24	1.07
A18	7.38 ± 0.24	3.06 ± 0.18	4.32 ± 0.24	3.78 ± 0.12	2.28 ± 0.12	4.32 ± 0.24	0.51
A19	5.88 ± 0.24	4.80 ± 0.24	1.08 ± 0.06	6.06 ± 0.18	1.98 ± 0.12	1.08 ± 0.06	1.03
A20	9.90 ± 0.36	6.54 ± 0.36	3.30 ± 0.12	5.58 ± 0.18	1.26 ± 0.06	3.30 ± 0.12	0.56
A21	19.62 ± 0.06	6.06 ± 0.30	13.56 ± 0.54	3.00 ± 0.18	0.48 ± 0.06	13.56 ± 0.54	0.15
A22	19.38 ± 0.72	7.98 ± 0.48	11.34 ± 0.54	1.98 ± 0.06	0.78 ± 0.06	11.34 ± 0.54	0.10
A23	19.14 ± 1.38	15.48 ± 1.38	3.66 ± 0.18	7.14 ± 0.48	1.14 ± 0.06	3.66 ± 0.18	0.37
$K_d$ (ml/g)	$\tau$ (days)						
$^{210}\text{Po}$	$^{210}\text{Pb}$	$^{210}\text{Pb}_t$	$^{210}\text{Po}_t$	$^{210}\text{Pb}_d$	$^{210}\text{Po}_d$	$^{210}\text{Pb}_p$	$^{210}\text{Po}_p$
9.1E+04	1.3E+04	41.8 ± 1.5	110.8 ± 3.2	34.9 ± 1.3	40.5 ± 1.3	6.8 ± 0.3	63.2 ± 3.2
4.7E+04	6.3E+04	46.2 ± 1.5	42.2 ± 0.6	24.9 ± 1.1	34.4 ± 0.8	21.2 ± 0.9	16.2 ± 0.6
2.3E+04	2.5E+04	105.0 ± 4.0	31.9 ± 0.9	86.0 ± 3.7	30.5 ± 1.1	18.8 ± 0.8	5.4 ± 0.0
6.4E+05	5.8E+04	41.9 ± 1.3	48.2 ± 1.9	22.4 ± 0.9	5.1 ± 0.0	19.4 ± 0.7	43.6 ± 1.9
1.3E+06	4.4E+04	92.2 ± 4.3	38.4 ± 1.6	73.0 ± 4.0	4.5 ± 0.0	19.1 ± 0.8	33.9 ± 1.6
1.4E+05	2.5E+05	25.1 ± 0.7	47.1 ± 1.6	10.8 ± 0.5	33.9 ± 1.0	14.2 ± 0.5	20.2 ± 0.8
1.9E+04	5.2E+04	47.9 ± 1.5	21.0 ± 0.0	31.7 ± 1.3	22.3 ± 0.0	16.1 ± 0.7	3.2 ± 0.0
9.0E+03	1.3E+05	62.9 ± 2.0	9.6 ± 0.6	31.5 ± 1.4	13.6 ± 0.9	31.3 ± 1.4	0.6 ± 0.0
4.9E+04	6.9E+04	80.9 ± 2.9	18.6 ± 0.5	58.3 ± 2.9	18.3 ± 0.7	22.5 ± 0.8	3.9 ± 0.0
2.1E+05	8.1E+04	27.1 ± 0.9	26.0 ± 0.8	17.9 ± 0.9	12.4 ± 0.8	9.2 ± 0.3	14.8 ± 0.7
3.2E+04	7.3E+04	13.9 ± 0.4	15.7 ± 0.6	7.0 ± 0.2	12.7 ± 0.7	7.0 ± 0.2	4.8 ± 0.0
3.5E+04	3.0E+04	55.3 ± 2.0	23.9 ± 0.7	43.0 ± 2.0	20.5 ± 0.8	12.2 ± 0.5	6.0 ± 0.0
2.0E+04	6.1E+04	64.6 ± 2.0	39.7 ± 1.4	38.3 ± 1.7	45.7 ± 2.0	26.2 ± 1.1	7.2 ± 0.0
2.4E+04	2.0E+04	17.3 ± 0.5	34.2 ± 0.9	7.4 ± 0.3	14.8 ± 1.0	9.9 ± 0.3	21.2 ± 0.9
2.6E+04	3.7E+04	22.9 ± 0.7	7.3 ± 0.0	14.1 ± 0.5	6.1 ± 0.0	8.7 ± 0.3	2.2 ± 0.0
3.2E+04	5.6E+04	46.9 ± 2.0	44.9 ± 1.7	31.3 ± 1.7	43.3 ± 2.2	15.5 ± 0.8	9.9 ± 0.8
1.2E+05	2.2E+04	28.6 ± 0.9	206.0 ± 9.1	9.9 ± 0.3	13.8 ± 0.9	18.7 ± 0.7	187. ± 9.1
4.3E+04	9.3E+04	23.9 ± 0.7	56.1 ± 1.7	9.9 ± 0.5	42.8 ± 2.2	14.0 ± 0.7	22.2 ± 0.8
3.1E+05	3.3E+04	28.5 ± 1.1	189.5 ± 5.6	23.2 ± 1.1	42.1 ± 2.5	5.2 ± 0.2	127. ± 5.6
NA	NA	47.7 ± 1.7	102.8 ± 3.3	31.6 ± 1.7	21.2 ± 1.0	16.0 ± 0.5	79.6 ± 3.3
5.1E+05	2.2E+05	95.2 ± 0.2	25.8 ± 1.5	29.2 ± 1.4	7.9 ± 0.9	65.8 ± 2.6	21.6 ± 1.5
1.7E+05	1.5E+05	93.7 ± 3.4	16.5 ± 0.5	38.5 ± 2.3	11.3 ± 0.8	54.9 ± 2.6	10.0 ± 0.0
6.0E+05	2.7E+04	92.5 ± 6.6	76.7 ± 5.1	74.7 ± 6.6	10.8 ± 0.5	17.7 ± 0.8	64.4 ± 5.1

NA: not available.

## References

- Roca Marti, M., Puigcorbe, V., Rutgers van der Loeff, M.M., Katlein, C., Fernández-Méndez, M., Peeken, I., Masqué, P., 2016. Carbon export fluxes and export efficiency in the central arctic during the record sea-ice minimum in 2012: a joint  $^{234}\text{Th}/^{238}\text{U}$  and  $^{210}\text{Po}/^{210}\text{Pb}$  study. *J. Geophys. Res. Oceans* 121, 5030–5049. <https://doi.org/10.1002/2016JC011816>.
- Bacon, M.P., Spencer, D.W., Brewer, P.G., 1976.  $^{210}\text{Pb}/^{226}\text{Ra}$  and  $^{210}\text{Po}/^{210}\text{Pb}$  disequilibria in seawater and suspended particulate matter. *Earth Planet. Sci. Lett.* 32, 277–296.
- Bacon, M.P., Brewer, P.G., Spencer, D.W., Murray, J.W., Goddard, J., 1980. Lead-210, polonium-210, manganese and iron in the Cariaco Trench. *Deep sea res. Part I. Oceanogr. Res. Rep.* 27, 119–135.
- Bacon, M.P., Belastock, R.A., Tecotzky, M., Turekian, K.K., Spencer, D.W., 1988. Lead-210 and polonium-210 in ocean water profiles of the continental shelf and slope south of New England. *Cont. Shelf Res.* 8, 841–853.
- Bai, Y., He, X., Pan, D., Chen, C.T.A., Kang, Y., Chen, X., Cai, W.J., 2014. Summertime

- Changjiang River plume variation during 1998–2010. *J. Geophys. Res. Oceans* 119 (9), 6238–6257.
- Baskaran, M., Santschi, P.H., 1993. The role of particles and colloids in the transport of radionuclides in coastal environments of Texas. *Mar. Chem.* 43, 95–114.
- Baskaran, M., Santschi, P.H., 2002. Particulate and dissolved  $^{210}\text{Pb}$  activities in the shelf and slope regions of the Gulf of Mexico waters. *Cont. Shelf Res.* 22, 1493–1510.
- Baskaran, M., Church, T., Hong, G., Kumar, A., Ma, Q., Choi, H., Rigaud, S., Maiti, K., 2013. Effects of flow rates and composition of the filter, and decay/in-growth correction factors involved with the determination of in situ particulate  $^{210}\text{Po}$  and  $^{210}\text{Pb}$  in seawater. *Limnol Oceanogr. Methods* 11, 126–138.
- Benninger, L.K., 1978.  $^{210}\text{Pb}$  balance in long Island sound. *Geochem. Cosmochim. Acta* 42, 1165–1174.
- Bian, C., Jiang, W., Greatbatch, R.J., 2013. An exploratory model study of sediment transport sources and deposits in the Bohai Sea, Yellow Sea, and East China Sea. *J. Geophys. Res. Oceans* 118, 5908–5923.
- Carvalho, F.P., 1997. Distribution, cycling and mean residence time of  $^{226}\text{Ra}$ ,  $^{210}\text{Pb}$  and  $^{210}\text{Po}$  in the Tagus estuary. *Sci. Total Environ.* 196, 151–161.
- Chang, P.H., Isobe, A., 2003. A numerical study on the Changjiang diluted water in the Yellow and East China Sea. *J. Geophys. Res. Atmos.* 108, 3299. <https://doi.org/10.1029/2002JC001749>.
- Cherry, M.I., Cherry, R.D., Heyraud, M., 1987. Polonium-210 and lead-210 in Antarctic marine biota and sea water. *Mar. Biol.* 96, 441–449.
- Church, T., Rigaud, S., Baskaran, M., Kumar, A., Friedrich, J., Masqué, P., Puigcorbó, V., Kim, G., Radakovic, O., Hong, G., Choi, H., Stewart, G., 2012. Intercalibration studies of  $^{210}\text{Po}$  and  $^{210}\text{Pb}$  in dissolved and particulate seawater samples. *Limnol Oceanogr. Methods* 10, 776–789.
- Fisher, N.S., Burns, K.A., Cherry, R.D., Heyraud, M., 1983. Accumulation and cellular distribution of  $^{241}\text{Am}$ ,  $^{210}\text{Po}$ , and  $^{210}\text{Pb}$  in two marine algae. *Mar. Ecol. Prog. Ser.* 11, 233–237.
- Guo, H., Zhang, S., Zhang, S., Lu, X., Li, S., 2017. Distribution and controls of heavy metals and organic matter in the surface sediments of the Southern Yellow Sea, China. *Environ. Sci. Pollut. Res.* 1–11. <https://doi.org/10.1007/s11356-017-9940-2>.
- Heyraud, M., Fowler, S.W., Beasley, T.M., Cherry, R.D., 1976. Polonium-210 in euphausiids: a detailed study. *Mar. Biol.* 34, 127–136.
- Higgo, J., Cherry, R.D., Heyraud, M., Fowler, S.W., Beasley, T., 1980. Vertical oceanic-transport of alpha-radioactive nuclides by zooplankton fecal pellets. In: *Natural Radiation Environment III. NTIS, CONF. pp.* 502–513.
- Honeyman, B.D., Santschi, P.H., 1989. A Brownian-pumping model for oceanic trace metal scavenging: Evidence from Th isotopes. *J. Mar. Res.* 47, 951–992.
- Honeyman, B.D., Santschi, P.H., 1992. The role of particles and colloids in the transport of radionuclides and trace metals in the oceans. In: Bufler, J., van Leeuwen, H.P. (Eds.), *Environmental Particles. IUPAC Series on Analytical and Physical Chemistry of Environ-Mental Systems*. Lewis, Boca Raton FL, pp. 379–423.
- Honeyman, B.D., Balistrieri, L.S., Murray, J.M., 1988. Oceanic trace metal scavenging: the importance of particle concentration. *Deep-Sea Res. Part I Oceanogr. Res. Pap.* 35, 227–246.
- Hong, G.H., Park, S.K., Baskaran, M., Kim, S.H., Chung, C.S., Lee, S.H., 1999. Lead-210 and polonium-210 in the winter well-mixed turbid waters in the mouth of the Yellow Sea. *Cont. Shelf Res.* 19, 1049–1064.
- Hong, G.H., Kim, Y.I., Baskaran, M., Kim, S.H., Chung, C.S., 2008. Distribution of  $^{210}\text{Po}$  and export of organic carbon from the euphotic zone in the southwestern East Sea (Sea of Japan). *J. Oceanogr.* 64, 277–292.
- Huang, D.K., Du, J.Z., Moore, W.S., Zhang, J., 2013. Particle dynamics of the Changjiang Estuary and adjacent coastal region determined by natural particle-reactive radionuclides ( $^7\text{Be}$ ,  $^{210}\text{Pb}$ , and  $^{234}\text{Th}$ ). *J. Geophys. Res. Oceans* 118, 1736–1748. <https://doi.org/10.1002/jgrc.20148>.
- Hung, G.W., Chung, Y.C., 1998. Particulate fluxes,  $^{210}\text{Pb}$  and  $^{210}\text{Po}$  measured from sediment trap samples in a canyon off northeastern Taiwan. *Cont. Shelf Res.* 18, 1475–1491.
- Jones, P., Maiti, K., McManus, J., 2015. Lead-210 and Polonium-210 disequilibria in the northern Gulf of Mexico hypoxic zone. *Mar. Chem.* 169, 1–15.
- Kim, G., 2001. Large deficiency of polonium in the oligotrophic ocean's interior. *Earth Planet. Sci. Lett.* 192, 15–21.
- Kim, Y., Yang, H.S., 2004. Scavenging of  $^{234}\text{Th}$  and  $^{210}\text{Po}$  in surface water of Jinhae Bay, Korea during a red tide. *Geochem. J.* 38, 505–513.
- Kim, S.H., Hong, G.H., Baskaran, M., Park, K.M., Chung, C.S., Kim, K.H., 1998. Wet removal of atmospheric  $^7\text{Be}$  and  $^{210}\text{Pb}$  at the Korean Yellow Sea coast. *The Yellow Sea* 4, 58–68.
- Kim, G., Ryu, J.W., Yang, H.S., Yun, S.T., 2005. Submarine groundwater discharge (SGD) into the Yellow Sea revealed by  $^{228}\text{Ra}$  and  $^{226}\text{Ra}$  isotopes: implications for global silicate fluxes. *Earth Planet. Sci. Lett.* 237, 156–166.
- Kim, H.C., Yamaguchi, H., Yoo, S., Zhu, J., Okamura, K., Kiyomoto, Y., Tanaka, K., Kim, S.W., Park, T., Oh, I.S., Ishizaka, J., 2009. Distribution of Changjiang diluted water detected by satellite chlorophyll-a and its interannual variation during 1998–2007. *J. Oceanogr.* 65 (1), 129–135.
- Lepore, K., Moran, S.B., Smith, J.N.H., 2009.  $^{210}\text{Pb}$  as a tracer of shelf-basin transport and sediment focusing in the Chukchi Sea. *Deep Sea Res. Part II Top. Stud. Oceanogr.* 56, 1305–1315.
- Liu, S.M., Hong, G.-H., Zhang, J., Ye, X.W., Jiang, X.L., 2009. Nutrient budgets for large Chinese estuaries. *Biogeosci. Discuss.* 6, 2245–2263.
- Liu, J.A., Su, N., Wang, X.L., Du, J.Z., 2017. Submarine groundwater discharge and associated nutrient fluxes into the Southern Yellow Sea: a case study for semi-enclosed and oligotrophic seas-implication for green tide bloom. *J. Geophys. Res. Oceans* 122, 139–152. <https://doi.org/10.1002/2016JC012282>.
- Ma, Q., 2013. Geochemical Behaviors of  $^{210}\text{Po}$  and  $^{210}\text{Pb}$  and Their Application in the China Marginal Seas. Doctoral Thesis. Xiamen University Press, Xiamen, China (in Chinese with English abstract).
- Ma, Q., Chen, M., Yang, W.F., Qiu, Y.S., Huang, Y.P., 2013.  $^{210}\text{Po}/^{210}\text{Pb}$  disequilibria in the surface waters of the north Pacific subtropical gyre. *J. Appl. Oceanogr.* 32, 3–12 (in Chinese with English abstract).
- Ma, H.Y., Yang, W.F., Zhang, L.H., Zhang, R., Chen, M., Chen, M., Qiu, Y.S., Zheng, M.F., 2017. Utilizing  $^{210}\text{Po}$  deficit to constrain particle dynamics in mesopelagic water, western South China Sea. *Geochem. Geophys. Geosyst.* 4, 1594–1607. <https://doi.org/10.1002/2017GC006899>.
- Marsan, D., Rigaud, S., Church, T., 2014. Natural radionuclides  $^{210}\text{Po}$  and  $^{210}\text{Pb}$  in the Delaware and Chesapeake Estuaries: modeling scavenging rate and residence times. *J. Environ. Radioact.* 138, 447–455.
- Masqué, P., Sanchez-Cabeza, J.A., Bruach, J.M., Palacios, E., Canals, M., 2002. Balance and residence times of  $^{210}\text{Pb}$  and  $^{210}\text{Po}$  in surface waters of the northwestern Mediterranean Sea. *Cont. Shelf Res.* 22, 2127–2146.
- Men, W., Liu, G.S., 2015. Distribution of  $^{226}\text{Ra}$  and the residence time of the shelf water in the Yellow Sea and the East China Sea. *J. Radioanal. Nucl. Chem.* 303, 2333–2344.
- Murray, J.W.B., Paul, B., Dunne, J.P., Chapin, T., 2005.  $^{234}\text{Th}$ ,  $^{210}\text{Pb}$ ,  $^{210}\text{Po}$  and stable Pb in the central equatorial Pacific: tracers for particle cycling. *Deep-Sea Res. Part I Oceanogr. Res. Pap.* 52, 2109–2139.
- Naimie, C.E., Blain, C.A., Lynch, D.R., 2001. Seasonal mean circulation in the Yellow Sea—a model-generated climatology. *Cont. Shelf Res.* 21, 667–695.
- Nozaki, Y., Tsunogai, S., 1976.  $^{226}\text{Ra}$ ,  $^{210}\text{Pb}$  and  $^{210}\text{Po}$  disequilibria in the western North Pacific. *Earth Planet. Sci. Lett.* 32, 313–321.
- Nozaki, Y., Tsubota, H., Kasemsupaya, V., Yashima, M., Naoko, I., 1991. Residence times of surface water and particle-reactive  $^{210}\text{Pb}$  and  $^{210}\text{Po}$  in the East China and Yellow seas. *Geochem. Cosmochim. Acta* 55, 1265–1272.
- Nozaki, Y., Dobashi, F., Kato, Y., Yamamoto, Y., 1998. Distribution of Ra isotopes and the  $^{210}\text{Pb}$  and  $^{210}\text{Po}$  balance in surface seawaters of the mid Northern Hemisphere. *Deep Sea Res. Part I Oceanogr. Res.* 45, 1263–1284.
- Quan, Q., Mao, X., Yang, X., Hu, Y., Zhang, H., Jiang, W., 2013. Seasonal variations of several main water masses in the southern Yellow Sea and East China Sea in 2011. *J. Ocean Univ. China* 12, 524–536. <https://doi.org/10.1007/s11802-013-2198-5>.
- Santschi, P.H., Li, H.Y., Bell, J., 1979. Natural radionuclides in the water of Narragansett bay. *Earth Planet. Sci. Lett.* 45, 201–213.
- Shannon, L.V., Cherry, R.D., Orren, M.J., 1970. Polonium-210 and lead-210 in the marine environment. *Geochem. Cosmochim. Acta* 34, 701–711.
- Stewart, G.M., Fowler, S.W., Teyssie, J.L., Cotret, O., Cochran, J.K., Fisher, N.S., 2005. Contrasting transfer of polonium-210 and lead-210 across three trophic levels in marine plankton. *Mar. Ecol. Prog. Ser.* 290, 27–33.
- Stewart, G.M., Cochran, J.K., Xue, J., Lee, C., Wakeham, S.G., Armstrong, R.A., Masqué, P., Miquel, J.C., 2007. Exploring the connection between  $^{210}\text{Po}$  and organic matter in the northwestern Mediterranean. *Deep-Sea Res. Part I Oceanogr. Res. Pap.* 54, 415–427.
- Su, N., Du, J.Z., Liu, S.M., Zhang, J., 2013. Nutrient fluxes via radium isotopes from the coast to offshore and from the seafloor to upper waters after the 2009 spring bloom in the Yellow Sea. *Deep Sea Res. Part II Top. Stud. Oceanogr.* 97, 33–42.
- Su, K., Du, J.Z., Baskaran, M., Zhang, J., 2017.  $^{210}\text{Po}$  and  $^{210}\text{Pb}$  disequilibrium at the PN section in the East China Sea. *J. Environ. Radioact.* 174, 54–65.
- Subha Anand, S., Rengarajan, R., Shenoy, D., Gauns, M., Naqvi, S.W.A., 2018. POC export fluxes in the Arabian Sea and the Bay of Bengal: a simultaneous  $^{234}\text{Th}/^{238}\text{U}$  and  $^{210}\text{Po}/^{210}\text{Pb}$  study. *Mar. Chem.* 198, 70–87. <https://doi.org/10.1016/j.marchem.2017.11.005>.
- Tang, Q.S., Zhang, J., Su, J.L., Tong, L., 2013. Spring blooms and the ecosystem processes: the case study of the Yellow Sea. *Deep Sea Res. Part II Top. Stud. Oceanogr.* 97, 1–3.
- Tateda, Y., Carvalho, F.P., Fowler, S.W., Miquel, J.C., 2003. Fractionation of  $^{210}\text{Po}$  and  $^{210}\text{Pb}$  in coastal waters of the NW Mediterranean continental margin. *Cont. Shelf Res.* 23, 295–316.
- Theng, T.L., Mohamed, C.A., 2005. Activities of  $^{210}\text{Po}$  and  $^{210}\text{Pb}$  in the water column at Kuala selangor, Malaysia. *J. Environ. Radioact.* 80, 273–286.
- Wang, Z., Yang, W.F., Chen, M., Lin, P., Qiu, Y.S., 2014. Intra-annual deposition of atmospheric  $^{210}\text{Pb}$ ,  $^{210}\text{Po}$  and the residence times of aerosol in Xiamen, China. *Aerosol Air Qual. Res.* 14, 1402–1410. <https://doi.org/10.4209/aaqr.2013.05.0170>.
- Wang, J.L., Zhang, W.G., Baskaran, M., Du, J.Z., Zhou, F., Wu, H., 2018. Fingerprinting sediment transport in river-dominated margins using combined mineral magnetic and radionuclide methods. *J. Geophys. Res. Oceans* 123, 5360–5374. <https://doi.org/10.1029/2018JC014174>.
- Wei, C.L., Murray, J.W., 1994. The behavior of scavenged isotopes in marine anoxic environments:  $^{210}\text{Pb}$  and  $^{210}\text{Po}$  in the water column of the Black Sea. *Geochem. Cosmochim. Acta* 58, 1795–1811.
- Wei, C.L., Lin, S.Y., Sheu, D.D.D., Chou, W.C., Yi, M.C., Santschi, P.H., Wen, L.S., 2011. Particle-reactive radionuclides ( $^{234}\text{Th}$ ,  $^{210}\text{Pb}$ ,  $^{210}\text{Po}$ ) as tracers for the estimation of export production in the South China Sea. *Biogeosci. Discuss.* 8, 3793–3808.
- Wei, C.L., Lin, S.Y., Wen, L.S., Sheu, D.D.D., 2012. Geochemical behavior of  $^{210}\text{Pb}$  and  $^{210}\text{Po}$  in the nearshore waters off western Taiwan. *Mar. Pollut. Bull.* 64, 214–220.
- Wei, C.L., Yi, M.C., Lin, S.Y., Wen, L.S., Lee, W.H., 2014. Seasonal distributions and fluxes of  $^{210}\text{Pb}$  and  $^{210}\text{Po}$  in the northern South China Sea. *Biogeosci. Discuss.* 11, 6813–6826.
- Wei, C.L., Chen, P.R., Lin, S.Y., Sheu, D.D., Wen, L.S., Chou, W.C., 2015. Distributions of  $^{210}\text{Pb}$  and  $^{210}\text{Po}$  in surface water surrounding Taiwan: a synoptic observation. *Deep Sea Res. Part II Top. Stud. Oceanogr.* 117, 155–166.
- Wu, Y., Zhang, J., Liu, S.M., Zhang, Z.F., Yao, Q.Z., Hong, G.H., Cooper, L., 2007. Sources and distribution of carbon within the Yangtze River system. *Estuar. Coast Shelf Sci.* 71, 13–25.
- Yang, C.Y., Lin, H.C., 1992. Lead-210 and polonium-210 across the frontal region between the Kuroshio and the East China sea, northeast of Taiwan. *Terr. Atmos. Ocean Sci.* 3, 379–394.

- Yang, W.F., Huang, Y.P., Chen, M., Zhang, L., Liu, H.B., Liu, G.S., Qiu, Y.S., 2006. Disequilibria between  $^{210}\text{Po}$  and  $^{210}\text{Pb}$  in surface waters of the southern South China Sea and their implications. *Sci. China Earth Sci.* 49, 103–112.
- Yi, Y., Bai, J., Liu, G.S., Yang, W.F., Yi, Q.T., Huang, Y.P., Chen, H.T., 2005. Measurements of atmospheric deposition fluxes of  $^7\text{Be}$ ,  $^{210}\text{Pb}$  and  $^{210}\text{Po}$ . *Mar. Sci.* 25, 20–24 (in Chinese with English abstract).
- Zhou, M.J., Liu, D.Y., Anderson, D.M., Valiela, I., 2015. Introduction to the special issue on green tides in the Yellow Sea. *Estuar. Coast Shelf Sci.* 163, 3–8. <https://doi.org/10.1016/j.ecss.2015.06.023>.
- Zhu, M.Y., Mao, X.H., Lü, R.H., Sun, M.H., 1993. Chlorophyll a and primary production in the Yellow Sea. *J. Oceanogr. Huanghai Bohai Seas* 11, 38–51 (in Chinese with English abstract).
- Zuo, Z., Esima, D., 1993.  $^{210}\text{Pb}$  and  $^{210}\text{Po}$  distributions and disequilibrium in the coastal and shelf waters of the southern North Sea. *Cont. Shelf Res.* 89, 999–1022.